

Adv-TGD: Adversarial Text-Guided Diffusion for Face Recognition Impersonation Attacks

OMID AHMADIEH, University of South Florida, Bellini College of Artificial Intelligence, Cybersecurity and Computing, USA

NIMA KARIMIAN*, University of South Florida, Bellini College of Artificial Intelligence, Cybersecurity and Computing, USA

The widespread adoption of face recognition (FR) technologies raises serious privacy concerns, as facial data can be exploited without consent. To address this challenge, we propose **Adv-TGD**, a generative adversarial attack framework that synthesizes photorealistic faces capable of impersonating target identities and deceiving face recognition systems. Built upon Stable Diffusion v2.1, Adv-TGD performs per-sample LoRA fine-tuning conditioned on concise textual prompts to generate natural yet adversarially manipulated identities. Unlike conventional identity-attack approaches, our method optimizes lightweight cross-attention adapters for each source–target pair within a single-step denoising process. Latent blending is constrained by a face-local heatmap mask to ensure spatially precise identity manipulation while preserving non-sensitive regions. We introduce a composite objective that integrates masked ϵ -MSE reconstruction, thresholded identity divergence in FR embedding space, directional feature alignment, and source-similarity suppression to balance adversarial attack and visual realism. Optionally, LLaVA-generated attribute prompts enhance fine-grained semantic details without reintroducing identity cues. Under the black-box evaluation protocol, **Adv-TGD** attains an average attack success rate (ASR) of **85.90%** across IR152, IRSE50, MobileFace, and FaceNet surpassing the semantic SOTA baseline Adv-CPG by **+6.25** points, diffusion-based makeup method DiffAIM by **+3** points, and noise-based P3-Mask by **+16** points. Despite its strong attack efficacy, Adv-TGD preserves high visual fidelity (**PSNR = 27.15 dB**, **SSIM = 0.981**). Furthermore, we demonstrate the flexibility of our framework by successfully extending it to in-the-wild datasets (LADN), general object classification (ImageNet), and transformer-based diffusion models (FLUX.1). These results demonstrate that text-guided, per-pair LoRA adaptation offers a practical and effective paradigm for adversarial face manipulation for impersonation attacks, unifying semantic controllability, photorealism, and robustness against unauthorized face recognition.

CCS Concepts: • **Security and privacy** → **Software and application security**; • **Computing methodologies** → **Machine learning**.

Additional Key Words and Phrases: Adversarial Generation, Stable Diffusion, Face identity manipulation, Latent Blending

ACM Reference Format:

Omid Ahmadih and Nima Karimian. 2026. Adv-TGD: Adversarial Text-Guided Diffusion for Face Recognition Impersonation Attacks. 1, 1 (June 2026), 24 pages. <https://doi.org/10.1145/nnnnnnn.nnnnnnn>

*Corresponding author: nkarimian@usf.edu

Authors' Contact Information: Omid Ahmadih, oa21@usf.edu, University of South Florida, Bellini College of Artificial Intelligence, Cybersecurity and Computing, Tampa, Florida, USA; Nima Karimian, nkarimian@usf.edu, University of South Florida, Bellini College of Artificial Intelligence, Cybersecurity and Computing, Tampa, Florida, USA.

Permission to make digital or hard copies of all or part of this work for personal or classroom use is granted without fee provided that copies are not made or distributed for profit or commercial advantage and that copies bear this notice and the full citation on the first page. Copyrights for components of this work owned by others than the author(s) must be honored. Abstracting with credit is permitted. To copy otherwise, or republish, to post on servers or to redistribute to lists, requires prior specific permission and/or a fee. Request permissions from permissions@acm.org.

© 2026 Copyright held by the owner/author(s). Publication rights licensed to ACM.

Manuscript submitted to ACM

Manuscript submitted to ACM

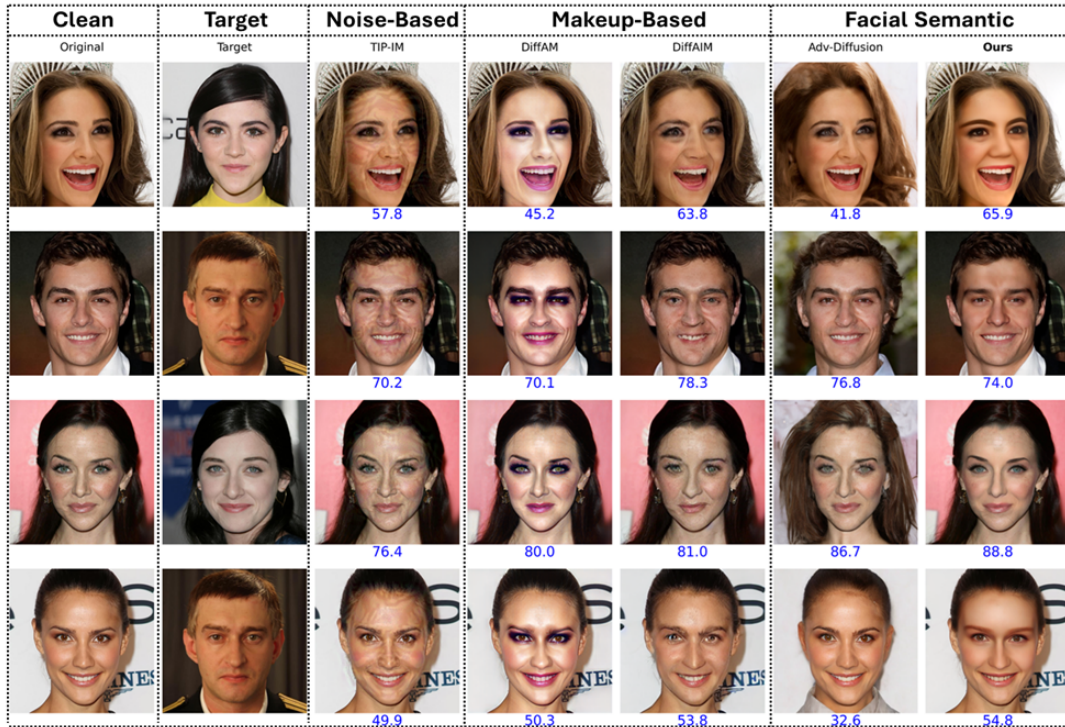


Fig. 1. The proposed **Adv-TGD** achieves realistic, identity-aligned face transformations while preserving texture, expression, and lighting consistency. The blue number above each image denotes the *Face++* confidence score.

1 Introduction

The rapid advancement of deep neural networks has propelled face recognition (FR) systems to remarkable success across applications such as authentication, surveillance, and social media tagging [31, 38]. However, their widespread deployment has raised serious privacy concerns. By exploiting large-scale public image datasets, FR models can infer social relationships [65], facilitate identity theft [53, 59], and even enable unauthorized mass surveillance [1]. Despite their impressive accuracy, modern face recognition systems remain vulnerable to adversarial manipulations. Understanding these vulnerabilities is critical for improving the robustness and security of biometric systems. In this work, we propose Adv-TGD, a diffusion-based adversarial attack framework that generates photorealistic facial images capable of impersonating target identities and deceiving multiple face recognition models. To counter these threats, adversarial attacks have emerged as a powerful defensive tool for adversarial attack. Early methods applied adversarial perturbations [4, 9, 32, 54, 60] to deceive FR models, but traditional noise-based [30, 61] and patch-based [10, 29, 50, 55–58, 62] attacks often produce visible artifacts, making them unsuitable for natural image sharing. A practical attack framework should protect identity while preserving photorealism. GAN-based editing [17, 28] improved realism via makeup transfer and semantic manipulation but required target-specific retraining and offered limited generalization within the GAN manifold. Diffusion models [22, 26, 27, 48, 49, 51] overcome these limits, providing high realism and controllability. Recent works—DiffProtect [27], Adv-Diffusion [26], and Adv-CPG [51]—pioneered diffusion-based

adversarial generation to protect facial privacy through latent perturbation and text-conditioned generation. However, they still rely on iterative optimization and target-specific fine-tuning, limiting efficiency and editability.

To address these limitations, we propose **Adv-TGD**, a text conditioned adversarial generation framework built on Stable Diffusion 2.1 (Fig. 2). Our model performs per-pair LoRA adaptation within the U-Net’s cross-attention layers, enabling single-step fine-tuning for each source–target identity pair while keeping the VAE, text encoder, and U-Net backbone frozen. As shown in Fig. 2, given a source image and a target identity, we utilize a hybrid **Saliency-Guided Semantic Mask (SGSM)** that fuses anatomical landmarks with aggregated FR gradients to localize identity-critical regions.

Within these regions, lightweight adapters are optimized to inject adversarial semantics guided by LLaVA-generated language prompts. Unlike traditional noise-based attacks, our framework targets low-to-mid frequency structural features, successfully neutralizing recognizers by dispersing their spatial attention—a process we quantify via spatial spread and entropy metrics. Text guidance is applied late and locally as a lightweight regularizer for attribute consistency (e.g., hair or accessories) rather than a primary driver of identity shift. Training uses a fixed diffusion step and *latent blending* so that FR models “see” the edited face on the original background; at inference, we invert the alignment and use seamless cloning (Normal Clone) to reinsert the result into the source frame, ensuring photorealistic reconstruction without edge artifacts or identity leakage.

In summary, our main contributions are:

- **Text-conditioned adversarial diffusion.** We present a diffusion-based impersonation framework that leverages natural-language guidance and lightweight LoRA adapters to generate adversarially shifted yet visually coherent identities. Our framework generate photorealistic impersonation images capable of deceiving multiple face recognition systems.
- **Automatic semantic prompt generation via vision language models.** We leverage LLaVA to automatically generate descriptive language prompts from the target image, enabling fine-grained semantic guidance for diffusion-based identity manipulation. This removes the need for manual prompt engineering while improving attribute consistency during adversarial face generation.
- **Saliency-Guided Semantic Masking (SGSM).** We introduce a hybrid masking strategy that integrates anatomical landmark priors with ensemble gradient saliency. By enforcing precise *top-k* spatial support within a semantic facial hull, SGSM selectively amplifies identity-critical regions and yields a contiguous, soft latent-space mask, achieving accurate identity localization without manual annotation.
- **Unified adversarial objective.** We develop a principled composite loss that integrates masked denoising, a threshold-aware softmin identity hinge, directional *source* \rightarrow *target* alignment, and source-suppression regularization. This formulation is designed to maximize spatial attention dispersion, forcing the recognizer to search a wider, non-identity-specific radius.
- **Cross-architecture attack generalization.** We show that Adv-TGD is architecture-agnostic and can be applied to both UNet-based diffusion models (Stable Diffusion 1.5 and 2.1) and transformer-based generative models (FLUX.1). Extensive experiments demonstrate that the proposed attack maintains strong impersonation success across different generative backbones, revealing a broader vulnerability of modern generative diffusion systems.
- **Realism and robustness.** We introduce a practical post-processing pipeline combining inverse alignment and seamless blending to restore natural context and eliminate boundary artifacts. The proposed approach preserves high visual fidelity (PSNR = 27.15 dB, SSIM = 0.981) while maintaining strong adversarial effectiveness, achieving

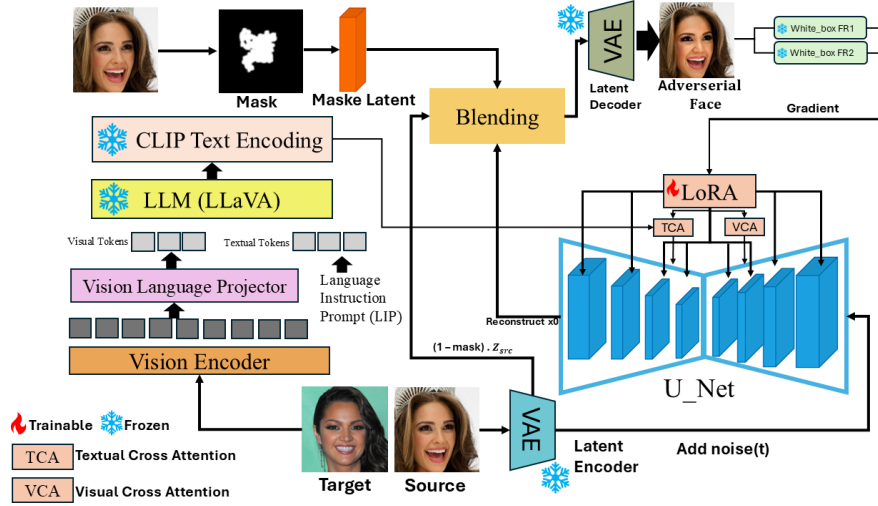


Fig. 2. **Architecture of Adv-TGD.** Per-pair LoRA fine-tuning on a frozen SD 2.1 U-Net with a single-step denoiser objective. A face-local SGSM produces a latent-resolution gate for masked latent blending; decoded images feed identity, directional, source-suppression, and late masked text losses. Re-evaluation blends the top-scoring aligned frame back into the original photo and reports ASR/PSNR/SSIM.

state-of-the-art impersonation performance with an average ASR of 85.90% across multiple face recognition models (IR152, IRSE50, MobileFace, and FaceNet).

2 Related Work

2.0.1 Diffusion Models for Semantic Image Manipulation. Diffusion models [6, 13, 41, 47] have revolutionized generative modeling by iteratively refining noise into coherent imagery. Latent formulations like Stable Diffusion [39, 41] enable semantically guided manipulation under text, mask, or structural control. Parameter-efficient adapters such as LoRA [14] and T2I-Adapters [33] add flexibility through low-rank updates without retraining the backbone. These properties make diffusion priors well-suited for adversarial face generation, where both realism and identity consistency are essential.

2.0.2 Text-Conditioned Personalization and Identity Adaptation. Text-conditioned personalization frameworks aim to retain individual identity while providing stylistic or semantic control through language [2, 16, 35, 40, 42, 43]. Recent approaches leverage adapter-based or prompt-tuning strategies [14, 24] to achieve rapid adaptation without retraining the entire model. However, most focus on visual customization rather than adversarial transformation. Our work revisits this paradigm, integrating LoRA-based textual conditioning with adversarial identity guidance to achieve semantically meaningful, stealthy adversarial impersonation. Given a target face I_{tgt} , LLaVA produces a textual description capturing high-level attributes such as hairstyle, facial structure, accessories, and appearance characteristics. The generated description is converted into a concise natural-language prompt c , which conditions the diffusion model during optimization. Unlike manual prompt engineering used in many text-guided diffusion methods, this automatic prompt generation ensures consistent semantic guidance while minimizing human intervention.

2.0.3 Adversarial Attacks for Face Recognition. Adversarial perturbations are widely used to bypass and evaluate unauthorized FR systems. Existing methods fall into *noise-based* and *unrestricted* categories. Noise-based approaches [3, 7, 8, 30, 46, 61] inject ℓ_p -bounded pixel noise or apply data poisoning and game-theoretic strategies to reduce recognition accuracy, but they often require model gradients or multiple samples and produce visible artifacts. Black-box variants like TIP-IM [61] relax these constraints yet still compromise realism. Unrestricted attacks embed perturbations in semantic edits [63], improving stealth but showing poor transferability and unnatural textures on unseen FR models.

2.0.4 Makeup-Based and Generative Adversarial Methods. Recent studies leverage facial makeup as a natural adversarial medium to conceal identity cues [15, 23, 37, 45, 63, 66]. By embedding adversarial signals within realistic cosmetic edits, these methods achieve high perceptual quality while preserving attack efficacy. However, reliance on large-scale makeup datasets introduces demographic bias and limits personalization when source and reference domains differ. Text-guided frameworks such as CLIP2Protect [44] mitigate these issues via semantic control but still inherit StyleGAN-related biases and limited cultural diversity [19, 34, 36, 64]. Moreover, most approaches rely on iterative optimization and lack strong generative priors for structure preservation; despite improved transferability from unrestricted and diffusion-based attacks, achieving consistently high ASR (proportion of generated images that are verified as the target identity by the recognition system) across models remains difficult.

2.0.5 Diffusion-Driven Adversarial Generation. Integrating diffusion priors into adversarial attack design has emerged as a strong alternative to pixel-space optimization. Adv-Diffusion [26] introduced latent perturbations but required multi-step optimization and lacked semantic control. Later variants such as Diffam [49] improved photorealism yet struggled to balance fidelity and adversarial strength. Our *Adv-TGD* advances this line by embedding text-guided, LoRA-based adaptation within Stable Diffusion 2.1’s cross-attention layers. It performs single-step, per-pair optimization with FR-aware masking and late textual regularization, achieving state-of-the-art ASR (Table 1) while maintaining contextual and identity realism. Motivated by the limitations of iterative or visually intrusive attacks, *Adv-TGD* serves as a unified, text-conditioned diffusion framework enabling fast, localized, and photorealistic identity impersonation.

3 Methodology

We introduce **Adv-TGD**, a per-sample LoRA fine-tuning framework that synthesizes *targeted* adversarial faces by adapting a frozen latent diffusion model with a lightweight, pair-specific adapter. The method has five ingredients: (i) a *face-local SGSM* that localizes edits to identity-bearing facial regions, (ii) *ensemble identity guidance* with a threshold-aware hinge aggregated by a softmin to remove weakest-view failure modes, (iii) a *directional identity* term that encourages movement toward the target in embedding space, (iv) *source suppression* to avoid snapping back to the source identity, and (v) a *late, masked text-image* loss to maintain attribute consistency. We train on aligned faces and seamlessly warp the result back into the original frame.

3.1 Preliminaries

3.1.1 Latent diffusion. We build on Stable Diffusion v2.1 [42] with encoder–decoder (\mathcal{E}, \mathcal{D}) and denoiser ϵ_θ acting on latents. For an image I , $z = \mathcal{E}(I)$ and $\hat{I} = \mathcal{D}(z)$. At noise index t with cumulative $\alpha_t \in (0, 1]$, we corrupt z to:

$$z_t = \alpha_t^{1/2} z + (1 - \alpha_t)^{1/2} \epsilon, \quad \epsilon \sim \mathcal{N}(0, I),$$

and predict $\hat{\epsilon}_\theta(z_t, t, c)$ under text condition c .

3.1.2 Parameter-efficient adaptation. For each source–target pair, we insert LoRA adapters into the U-Net cross-attention projections (to_q, to_k, to_v, to_out.0) and optimize only those parameters. The VAE, text encoder, and the base U-Net remain frozen.

3.2 Overview

Given a source I_{src} and a target I_{tgt} , we (1) align both faces and construct a soft, identity-aware mask M ; (2) fine-tune a pair-specific LoRA via a single-step denoiser objective with latent blending guided by M^ℓ (latent-resolution mask); and (3) invert the alignment and apply seamless blending to insert the edited face back into the original photo.

3.3 Saliency-Guided Semantic Masking (SGSM)

To ensure that adversarial perturbations are both effective and spatially constrained, we propose a hybrid masking strategy that fuses anatomical priors with model-specific sensitivity. Let $\{\mathcal{F}_k\}_{k=1}^K$ denote an ensemble of FR models.

On the aligned source image \mathbf{x}_s , we first define a *semantic prior* M_{sem} as a landmark-based convex hull covering the eyes, nose, mouth, and jawline. Simultaneously, we derive a *target-aware saliency map* S by backpropagating the cosine similarity toward the target embedding:

$$S = \frac{1}{K} \sum_{k=1}^K \left| \nabla_{\mathbf{x}_s} \cos(\mathcal{F}_k(\mathbf{x}_s), e_{\text{tgt}}^k) \right|. \quad (1)$$

The raw saliency is gated by an elliptical face prior $P \in [0, 1]^{H \times W}$ and normalized. The final hybrid mask M is defined as the union of the semantic prior and the top- $p\%$ most salient regions, followed by morphological dilation and Gaussian feathering:

$$M = \text{Feather}(M_{\text{sem}} \cup \text{TopK}(S, p\%)). \quad (2)$$

This hybrid approach ensures the optimizer targets specific identity-bearing structures (via S) while remaining strictly bounded by facial anatomy (via M_{sem}), preventing background artifacts or “ghosting” often seen in unconstrained adversarial edits. The mask is downsampled to $M^\ell \in [0, 1]^{H/8 \times W/8}$ to guide the latent-space blending.

3.4 Single-Step Diffusion Denoising with LoRA Optimization

At each iteration we form a single noisy latent slice from the aligned source, predict noise with the LoRA-augmented UNet, reconstruct a clean latent, blend it with the source using a face mask, and decode to the image; only the LoRA weights are updated.

Form a noisy latent and predict noise:

$$z_{\text{src}} = \mathcal{E}(I_{\text{src}}), \quad \epsilon \sim \mathcal{N}(0, I), \quad (1a)$$

$$z_t = \alpha_t^{1/2} z_{\text{src}} + (1 - \alpha_t)^{1/2} \epsilon, \quad (1b)$$

$$\hat{\epsilon}_\theta = \text{UNet}_{\text{LoRA}}(z_t, t, c). \quad (1c)$$

where \mathcal{E} is the VAE encoder; I_{src} is the aligned source face; $t = \lfloor \tau t_{\text{max}} \rfloor$ uses a fixed diffusion index fraction $\tau \in (0, 1)$; α_t is the scheduler’s cumulative noise factor; c is the text conditioning; $\text{UNet}_{\text{LoRA}}$ is the frozen UNet with trainable LoRA in cross-attention.

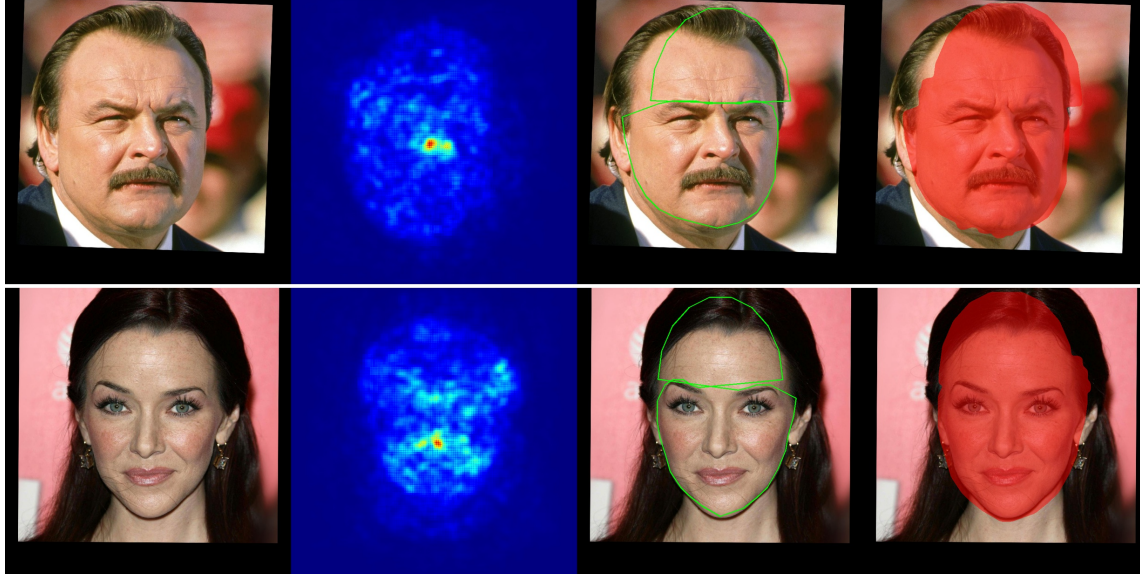


Fig. 3. **Salience-Guided Semantic Masking (SGSM)**. Comparison across two identities showing (Col 1) Source, (Col 2) Saliency hotspots S , (Col 3) Semantic hull M_{sem} , and (Col 4) the final hybrid mask M . The strategy ensures targeted identity manipulation while maintaining anatomical grounding.

Reconstruct the clean latent according to the scheduler type:

$$\epsilon\text{-pred: } \hat{z}_0 = (z_t - (1 - \alpha_t)^{1/2} \hat{\epsilon}_\theta) / \alpha_t^{1/2}, \quad (2a)$$

$$v\text{-pred: } \hat{z}_0 = \alpha_t^{1/2} z_t - (1 - \alpha_t)^{1/2} \hat{\epsilon}_\theta. \quad (2b)$$

where the chosen case matches the diffusion scheduler's prediction parameterization.

Blend only the facial region in latent space and decode:

$$\hat{z}_0^{\text{blend}} = M^\ell \odot \hat{z}_0 + (1 - M^\ell) \odot z_{\text{src}}, \quad (3a)$$

$$\hat{I} = \mathcal{D}(\hat{z}_0^{\text{blend}}). \quad (3b)$$

where $M^\ell \in [0, 1]^{H^\ell \times W^\ell}$ is the latent-resolution face mask; \odot is element-wise multiply; \mathcal{D} is the VAE decoder; \hat{I} is used by the losses in 3.5.

Update step (LoRA only):

$$\theta_{\text{LoRA}} \leftarrow \theta_{\text{LoRA}} - \eta \nabla_{\theta_{\text{LoRA}}} \mathcal{L},$$

where θ_{LoRA} are just the LoRA weights; η is the learning rate. The VAE (\mathcal{E} , \mathcal{D}), text encoder, and base UNet remain frozen.

Algorithm 1 Single-step LoRA fine-tuning (per source–target pair)

Require: aligned $(I_{\text{src}}, I_{\text{tgt}})$, text c , masks M, M^ℓ , FR ensemble $\{\mathcal{F}_k\}$, fixed index t

- 1: $z_{\text{src}} \leftarrow \mathcal{E}(I_{\text{src}})$; sample $\epsilon \sim \mathcal{N}(0, I)$
 - 2: $z_t \leftarrow \alpha_t^{1/2} z_{\text{src}} + (1 - \alpha_t)^{1/2} \epsilon$
 - 3: $\hat{\epsilon}_\theta \leftarrow \text{UNet}_{\text{LoRA}}(z_t, t, c)$
 - 4: reconstruct \hat{z}_0 from $(z_t, \hat{\epsilon}_\theta)$ using Eq. (3)
 - 5: $\hat{z}_0^{\text{blend}} \leftarrow M^\ell \odot \hat{z}_0 + (1 - M^\ell) \odot z_{\text{src}}$; $\hat{I} \leftarrow \mathcal{D}(\hat{z}_0^{\text{blend}})$
 - 6: compute losses $\mathcal{L}_\epsilon, \mathcal{L}_{\text{id}}, \overline{\mathcal{D}}, \overline{\mathcal{S}}, \mathcal{L}_{\text{txt}}$
 - 7: update **LoRA parameters only**; keep VAE, text encoder, base UNet frozen
-

3.5 Losses and Regularizers

3.5.1 FR Embedding Notation and Cosine Operators. Before introducing the losses, we fix notation and define the quantities used throughout. We use the cosine similarity and the unit-normalization operator:

$$\cos(u, v) = \frac{\langle u, v \rangle}{\|u\| \|v\|}, \quad \nu(x) = \frac{x}{\|x\|}. \quad (4)$$

Given an ensemble of K face recognizers $\{\mathcal{F}_k\}_{k=1}^K$, we denote the *unit-normalized* embeddings of the (aligned) source image I_{src} , target image I_{tgt} , and the current prediction \hat{I} as:

$$e_{\text{src}}^k = \nu(\mathcal{F}_k(I_{\text{src}})), \quad e_{\text{tgt}}^k = \nu(\mathcal{F}_k(I_{\text{tgt}})), \quad f_k(\hat{I}) = \nu(\mathcal{F}_k(\hat{I})). \quad (5)$$

All identity terms below are computed with these normalized embeddings.

3.5.2 Training objective. We combine a masked denoising term with identity guidance, directional consistency, source suppression, and a late text prior. The identity-related terms are smoothly ramped during training, while text guidance activates in later iterations:

$$\mathcal{L} = \lambda_\epsilon \mathcal{L}_\epsilon + s(i)(\lambda_{\text{id}} \mathcal{L}_{\text{id}} + \lambda_{\text{dir}} \overline{\mathcal{D}} + \lambda_{\text{src}} \overline{\mathcal{S}}) + \lambda_{\text{txt}}(i) \mathcal{L}_{\text{txt}}. \quad (6)$$

where $\lambda_\epsilon, \lambda_{\text{id}}, \lambda_{\text{dir}}, \lambda_{\text{src}}$ are fixed weights, $s(i) = b + (1 - b)(i/N)^y$ ramps identity terms over iteration i , and $\lambda_{\text{txt}}(i)$ turns on the text prior in the late phase.

3.5.3 Latent-Space Masked Denoising Loss. We restrict the denoising objective to the facial latent region so capacity is focused where identity resides:

$$\mathcal{L}_\epsilon = \frac{1}{Z} \sum_{c,i,j} M_{ij}^\ell (\epsilon_{cij} - \hat{\epsilon}_{\theta,cij})^2, \quad Z = C \sum_{i,j} M_{ij}^\ell. \quad (7)$$

where $M^\ell \in [0, 1]^{H^\ell \times W^\ell}$ is the latent-resolution face mask, C is the latent channel count, ϵ is the sampled noise, and $\hat{\epsilon}_\theta$ is the UNet prediction at (z_t, t, c) .

3.5.4 Verification-Based Identity Loss (Ensemble). We encourage the generated face to be verified as the target by several FR models by pushing its similarity to each model’s target embedding above a standard threshold.

$$s_k = \cos(f_k(\hat{I}), e_{\text{tgt}}^k), \quad (8)$$

$$\mathcal{L}_{\text{id}} = \frac{1}{K} \sum_{k=1}^K [(\tau_k + \Delta) - s_k]_+. \quad (9)$$

where $f_k(\hat{I})$ is the FR embedding of the generated image under model \mathcal{F}_k (unit-normalized), e_{tgt}^k is the unit-normalized target embedding, s_k is their cosine similarity, τ_k is the verification threshold for \mathcal{F}_k , $\Delta > 0$ is a small safety margin, and $[x]_+ = \max(x, 0)$.

3.5.5 Directional identity (move along source \rightarrow target displacement). We encourage updates that follow the identity change from the source to the target in FR embedding space, rather than exploiting superficial shortcuts.

$$\begin{aligned} u_k &= \nu(f_k(\hat{I}) - e_{\text{src}}^k), & v_k &= \nu(e_{\text{tgt}}^k - e_{\text{src}}^k), \\ \mathcal{D}_k &= 1 - \cos(u_k, v_k), & \overline{\mathcal{D}} &= \frac{1}{K} \sum_{k=1}^K \mathcal{D}_k. \end{aligned} \quad (10)$$

where $f_k(\hat{I})$ is the unit-normalized embedding of the current prediction under FR model \mathcal{F}_k ; e_{src}^k and e_{tgt}^k are the unit-normalized embeddings of source and target; u_k is the *observed* change (prediction minus source), v_k is the *desired* source \rightarrow target displacement, and $1 - \cos(u_k, v_k)$ penalizes misalignment.

3.5.6 Source suppression (avoid regress-to-source). We discourage the optimizer from drifting back toward the original identity once progress toward the target has been made.

$$\mathcal{S}_k = [\cos(f_k(\hat{I}), e_{\text{src}}^k) - m]_+, \quad \overline{\mathcal{S}} = \frac{1}{K} \sum_{k=1}^K \mathcal{S}_k. \quad (11)$$

where $f_k(\hat{I})$ is the unit-normalized embedding of the current prediction under FR model \mathcal{F}_k ; e_{src}^k is the unit-normalized source embedding; and $m \in [0, 1)$ is a small margin tolerance.

3.5.7 CLIP-Based Semantic Alignment. To maintain high-level semantic agreement with the textual prompt while avoiding global drift, we introduce a weak CLIP-guided prior applied only to the facial region:

$$\mathcal{L}_{\text{txt}} = 1 - \cos(\phi_{\text{img}}(\text{crop}(\hat{I}, M)), \phi_{\text{text}}(c)). \quad (12)$$

where ϕ_{img} and ϕ_{text} are CLIP-family image/text encoders, and $\text{crop}(\hat{I}, M)$ uses the image-space face mask M to ensure the comparison focuses exclusively on facial content. We apply this term only in the later stage of optimization via $\lambda_{\text{txt}}(i)$, once identity and denoising have stabilized.

3.5.8 Schedules and timestep. Identity terms use $s(i)$ above; the text weight $\lambda_{\text{txt}}(i)$ activates late; training uses a fixed diffusion index fraction τ for stability.

3.6 Post-processing: inverse alignment and seamless blending

Because training operates in a canonical, tightly aligned facial coordinate frame, the edited output must be mapped back to the original image geometry. We first apply the inverse of the alignment affine transform (estimated from facial landmarks) to warp the edited face back to its native pose, scale, and position. This step restores the global structure of the image and ensures spatial consistency with the source context.

However, latent edits may introduce low-frequency tone shifts or local inconsistencies along the face boundary. To mitigate these artifacts, we perform Poisson seamless cloning using the warped prediction as the foreground and the original image as the background. This gradient-domain blending harmonizes illumination, suppresses hard edges, and preserves the background’s high-frequency detail while keeping the edited facial region intact. Crucially, we utilize standard Alpha blending or Poisson Normal cloning rather than Mixed cloning; as our ablation study demonstrates,

Table 1. Attack Success Rate (ASR%) on FFHQ and CelebA-HQ

Category	Method	FFHQ				CelebA-HQ				Avg.
		IR152	IRSE50	FaceNet	Mobile	IR152	IRSE50	FaceNet	Mobile	
	Clean	3.20	2.20	2.10	4.90	2.10	5.61	0.80	13.60	4.31
Noise-Based	TI-DIM [8]	42.26	63.91	14.28	51.71	34.08	60.51	13.27	51.25	41.41
	TIP-IM [61]	44.86	65.36	58.03	50.47	40.02	55.57	37.90	48.07	50.04
	P3-Mask [5]	70.98	82.79	56.18	68.57	71.27	80.90	58.43	67.55	69.58
Makeup / Attribute	CLIP2Protect [44]	50.56	83.93	43.66	74.00	46.20	78.53	41.29	71.43	61.20
	DFPP [45]	52.62	87.91	50.57	77.69	45.00	78.37	44.01	69.97	63.24
	DiffAM [49]	65.22	87.59	63.01	86.87	62.14	86.97	61.10	81.97	74.49
	DiffAIM [52]	<u>82.20</u>	<u>91.04</u>	68.21	<u>94.21</u>	<u>80.56</u>	<u>90.37</u>	64.14	<u>93.10</u>	<u>82.85</u>
Portrait / Semantic	Adv-Diffusion [26]	49.40	79.31	29.91	65.49	51.25	79.22	33.90	68.66	57.14
	Adv-CPG [51]	75.26	91.03	62.84	89.94	76.96	88.72	<u>63.50</u>	87.95	79.65
	TCA ² [25]	53.63	77.31	41.62	72.21	52.50	76.21	40.72	71.92	60.76
	Adv-TGD (Ours)	88.80	94.60	<u>63.40</u>	95.40	90.60	94.80	63.40	96.20	85.90

the latter’s tendency to preserve source image gradients which contain high-frequency identity-bearing textures can inadvertently restore the original identity and nullify the attack.

In practice, this two-stage post-processing substantially improves visual fidelity by (i) respecting the original scene geometry, (ii) avoiding boundary halos caused by the VAE decoder, and (iii) ensuring that the final output remains photorealistic under arbitrary lighting and backgrounds.

4 Experiments

In this work, we operate under a realistic transfer-based black-box setting for the final victim system, while leveraging a white-box setting during the optimization of our surrogate ensemble. Specifically, we assume the attacker does not have access to the target system. Instead, we utilize the gradients of a surrogate ensemble consisting of other three models to optimize the adversarial features. The potency of DiffAttack relies on the cross-model transferability of these latent-space perturbations. We evaluate the effectiveness of our method in *black-box* attack settings against robust face recognition (FR) models and compare with recent state-of-the-art. We also report perceptual fidelity metrics and ablations of key components.

4.1 Experimental Setting

4.1.1 Dataset. We evaluate Adv-TGD using two widely adopted, high-quality facial image datasets: CelebA-HQ [20] and FFHQ [21]. In line with the protocol described in [26, 51], a subset of 1,000 face images representing distinct identities is selected from each dataset along with five more images as a target image. The 1,000 face images are divided into five groups, with five target images randomly chosen per group. As a result, each dataset contains five groups, each comprising 200 source–target image pairs.

4.1.2 Implementation details. We build on Stable Diffusion v2.1 at 768×768. For each (I_{src}, I_{tgt}) pair, we fine-tune a *pair-specific* LoRA adapter injected into U-Net cross-attention projections to_q, to_k, to_v, to_{out}. \emptyset . We use LoRA rank $r = 16$ and $\alpha = 64$ with dropout 0.08. Training runs for 65 steps (AdamW, base LR 3×10^{-5} with late linear decay to 1×10^{-5}). We use a single denoising slice per step with a fixed time index fraction $\tau = 0.6$, DDPM scheduler, and latent

blending under a soft face mask. OpenCLIP text guidance is applied only in the late phase, and perceptual/TV terms are weak and masked to the face region. Re-evaluation scores are computed after seamless blending back into the original frame.

4.1.3 Evaluation Metrics. We evaluate our approach by independently assessing attack performance and image quality. To measure attack performance, we adopt the Attack Success Rate (ASR) [18, 26, 51], which quantifies the proportion of adversarial examples that successfully deceive the target model:

$$\text{ASR} = \frac{1}{K} \sum_I \mathbb{I}(\cos(h(I_t), h(I_{adv})) > \tau) \times 100\%, \quad (13)$$

where \mathbb{I} denotes the indicator function, K represents the total number of face images, and τ is the decision threshold. I_t and I_{adv} correspond to the target and adversarial face images, respectively. The threshold τ is set to yield a 0.01 False Acceptance Rate (FAR) for each victim model, following the same configuration as [18, 26, 51]. For image quality assessment, we employ three standard metrics: Frechet Inception Distance (FID), Peak Signal-to-Noise Ratio (PSNR), and Structural Similarity Index (SSIM).

4.2 Comparison with SOTA Methods

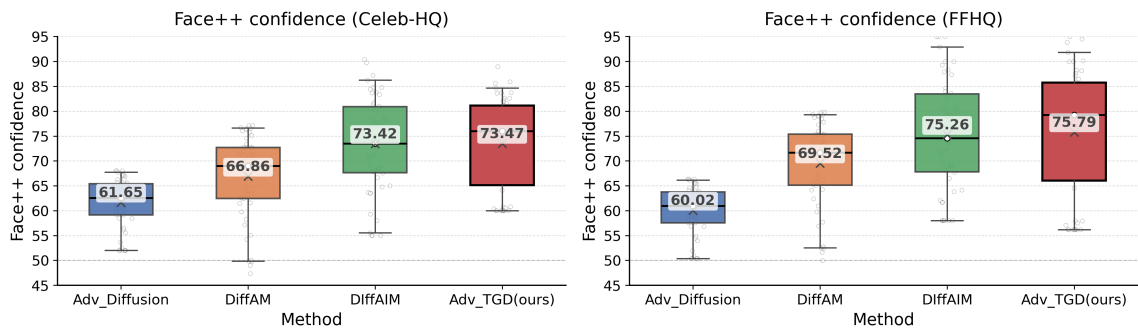
4.2.1 Quantitative results. Table 1 summarizes the attack success rates (ASR) under the black-box setting; underlined entries denote the highest value in each column. For face verification, we set the decision threshold τ per model at FAR = 0.01. Our method achieves strong black-box transferability, particularly on IR152, IRSE50, and MobileFace, and substantially outperforms representative noise-, makeup-, and semantic-based baselines. To further validate the imperceptibility of the proposed adversarial attack, we evaluate the visual quality of adversarial examples compared with representative SOTA baselines. Following common practice, we adopt Frechet Inception Distance (FID) [12], Peak Signal-to-Noise Ratio (PSNR), and Structural Similarity Index (SSIM) as evaluation metrics. Table 2 reports the quantitative results aggregated across multiple runs. While Adv-Diffusion and DiffAIM achieve lower FID scores, our method achieves the highest SSIM (0.981) and highest PSNR (27.15 dB). This indicates that while baseline methods may match the unconditional image distribution slightly better, **Adv-TGD** significantly outperforms them in pixel-level structural preservation. For stealthy adversarial impersonation, this structural and spatial consistency is arguably more critical to ensure seamless facial blending and minimal visual distortion.

4.2.2 Image quality assessment. To evaluate the visual imperceptibility of the proposed adversarial generation framework, we further analyze the perceptual quality of generated images. In general, lower FID values indicate that the generated images are closer to the real image distribution, while higher PSNR and SSIM values correspond to better reconstruction fidelity and structural consistency. In addition to quantitative evaluation, we also present qualitative comparisons in Fig. 1. The results show that Adv-TGD produces visually coherent faces that preserve lighting, expression, and background consistency while successfully aligning with the target identity. Compared with existing approaches, our method introduces fewer visual artifacts and maintains more natural facial appearance, highlighting the effectiveness of the proposed semantic-guided adversarial generation framework.

4.2.3 Evaluation on commercial FR API. To assess black-box transferability under a real-world deployment scenario, we further evaluate all methods on a production-grade commercial face verification service. For each dataset (CelebA-HQ and FFHQ), we sample 100 source–target identity pairs and generate a adversarial source image for every method. Each adversarial image is then submitted to the Face++ *Compare* API together with its corresponding target image. The

Table 2. Perceptual quality comparison. Lower is better for FID; higher is better for PSNR/SSIM.

Method	FID↓	PSNR↑	SSIM↑
TIP-IM	38.73	33.21	0.924
Adv-Diffusion	22.58	28.85	0.805
DiffAM	26.10	20.53	0.886
Adv-CPG	26.07	29.99	0.897
DiffAIM	23.23	25.39	0.739
Adv-TGD (Ours)	27.26	27.15	0.981

Fig. 4. Face++ confidence scores (\uparrow) returned from the commercial API for four attack methods on **CelebA-HQ** (left) and **FFHQ** (right).

API returns a proprietary confidence score in $[0, 100]$ that reflects the similarity between the two inputs, where larger values indicate stronger impersonation. Visualization of the empirical distributions is provided in Fig. 4.

5 Ablation Study and Mechanism Analysis

To rigorously evaluate the contribution of each component in our **Adv-TGD** framework, we conduct a comprehensive ablation study using a leave-one-out strategy. Experiments are performed on a randomly sampled subset of the CelebA-HQ dataset using the industry-standard **IR152** recognizer at **FAR=0.01**. The results in Table 3 highlight the trade-offs between identity manipulation effectiveness (Attack Success Rate – ASR), visual fidelity (PSNR, SSIM), and computational efficiency.

Table 3. **Ablation analysis of Adv-TGD on CelebA-HQ.** We evaluate different masking strategies, loss components, and blending techniques. Runtime is measured as the average time to generate one adversarial example on a single NVIDIA A100 GPU. Our proposed **SGSM** achieves the best balance between adversarial effectiveness and visual fidelity.

Variant	ASR (%) ↑	PSNR ↑	SSIM ↑	Runtime (s) ↓	Observation
<i>Masking Strategies</i>					
Saliency Mask	77.50	27.84	0.984	85.2	High fidelity but weaker identity manipulation.
Full Image Editing	90.50	23.54	0.958	42.4	Strong attack but severe background distortion.
Geometric Mask	89.50	25.29	0.968	36.7	Landmark constraint improves structural edits.
SGSM (Ours)	91.00	26.53	0.979	98.1	Best attack–quality trade-off.
<i>Loss Components</i>					
w/o Directional Loss (L_{dir})	87.20	26.41	0.985	84.9	Less consistent identity shift.
w/o Source Suppression (L_{src})	85.60	26.38	0.984	85.1	Source identity partially preserved.
w/o Text Guidance (L_{txt})	89.80	26.47	0.984	83.5	Slight drop in semantic consistency.
<i>Blending Strategies</i>					
Mixed Poisson Blending	31.50	25.08	0.977	36.6	Preserves source texture and restores identity.
Laplacian Pyramid Blending	90.00	26.18	0.977	112.4	Similar performance but higher cost.

5.1 Impact of Masking Strategy

The masking strategy is the most influential factor in our pipeline. The **Saliency-Only Mask** baseline utilizes only the FR model’s attention maps; while it preserves high visual quality, it often fails to cover identity-leaking features that the model deems non-salient (e.g., specific jawline structures), resulting in a lower ASR of 77.5%. **No Masking** (Full Image Editing) yields a high ASR (90.5%) but drastically degrades fidelity by destroying background consistency. The **Parsing Mask** (Geometric Mask) utilizes a landmark-based convex hull to strictly mask the anatomical face, achieving a strong ASR of 89.5%; this confirms that geometric constraints force the optimizer to make structural changes rather than relying on superficial background noise. Our proposed **SGSM** achieves the optimal **ASR of 91.0%** by fusing anatomical landmarks with target-aware gradients, ensuring the optimizer targets specific identity-bearing “hotspots” while maintaining superior fidelity.

5.2 Impact of Loss Components and Text Guidance

Removing the **Directional Loss** (L_{dir}) lowers the mean cosine similarity (0.228 vs 0.231), validating its role in steering the identity shift along the semantic vector in embedding space rather than just pushing it away randomly. When using only a basic hinge loss without the directional term, we observe that some adversarial examples partially drift between source and target identities, especially under challenging poses. In the absence of **Source Suppression** (L_{src}), the optimizer tends to “snap back” to source identity features, highlighting L_{src} as a critical anchor. **Text Guidance** (L_{txt}) acts as a semantic regularizer; removing it results in a slight decrease in semantic consistency, confirming its effectiveness as a lightweight refinement once identity and denoising have stabilized. Furthermore, applying strong text guidance from the beginning may overemphasize textual attributes at the expense of identity stability, demonstrating why our late-stage application is necessary.

5.3 Impact of Blending Techniques

Mixed Poisson Blending creates a massive failure case (ASR drops to 31.5%) because mixed cloning attempts to preserve the gradient structure of the source image. Since identity is heavily encoded in high-frequency texture details

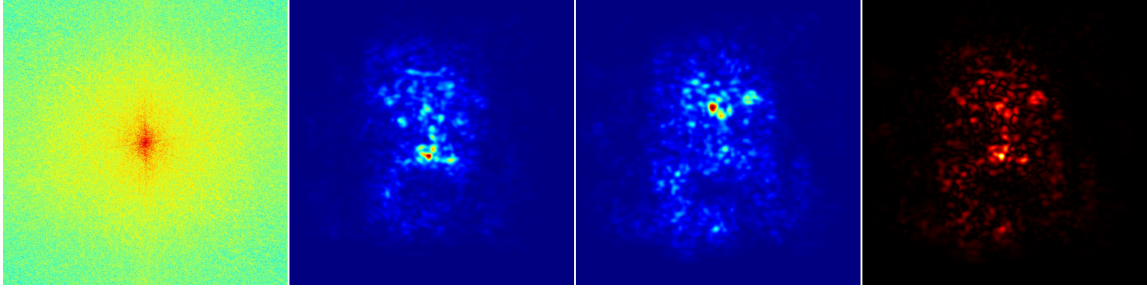


Fig. 5. **Mechanism of Identity Neutralization.** From left to right: (1) spectral analysis confirming the attack targets structural frequencies. (2-3) visualization of FR focal attention dispersal. (4) saliency difference map $|S_{adv} - S_{src}|$, revealing the precise anatomical regions neutralized by **Adv-TGD**.

(pores, wrinkles), preserving source gradients inadvertently reconstructs the original identity. **Laplacian Pyramid Blending** performed similarly to our final model (90.0% ASR) but is computationally more expensive. Thus, we utilize Gaussian-feathered alpha blending as it provides the optimal balance of efficiency and quality.

5.4 Visual and Spectral Analysis

To investigate the mechanism of the identity shift, we perform a spatial and frequency-domain analysis of the generated adversarial perturbations.

5.4.1 Attention Disruption and Dispersion. Fig. 5(b-d) visualizes the FR model’s attention maps. While the source image triggers concentrated activations tightly clustered around identity-critical landmarks (e.g., ocular and nasal regions), **Adv-TGD** successfully neutralizes the recognizer by dispersing its spatial attention. We quantify this effect by measuring the spatial spread (RMS variance) and informational entropy. In notable instances, our method can expand the spatial spread of the model’s attention by up to **8.4%** while increasing spatial entropy by as much as **1.5%**. As shown in the difference map (Fig. 5d), the attack does not simply add noise but systematically dismantles the focal points required for identification.

5.4.2 Frequency Domain Analysis. Fig. 5(a) displays the Discrete Fourier Transform (DFT) of the perturbation. The energy is heavily concentrated in the low-to mid frequency bands (central region), indicating that the attack targets semantic facial structures, such as jawline geometry and facial depth, rather than relying on high-frequency pixel noise. This structural nature explains the failure of **Mixed Poisson Blending**; by attempting to preserve the source image’s gradient structure, Mixed Blending inadvertently restores the original identity’s low-frequency structural signal, nullifying the adversarial effect.

5.5 Optimization Dynamics

To further understand the generative process, we visualize the evolution of the adversarial face during the per-pair LoRA optimization. Fig. 6 illustrates the progression across 100 optimization steps for multiple source–target pairs. In the early stages (e.g., Step 20), the optimizer begins altering the foundational facial geometry and low-frequency depth cues. As training progresses, fine-grained identity features such as the jawline, eye shape, and skin textures are aggressively refined to match the target. The *Final* row demonstrates the result of our post-processing pipeline, where

the optimized adversarial face is seamlessly blended back into the original source lighting and background context, yielding a high-fidelity, adversarial image.

6 Experimental Prompts

Fig. 7 displays example text used to generate the adversarial examples shown in experiments. These texts are descriptive yet broad enough to allow the optimization to dictate facial structure. The specific prompt used to generate these textual descriptions is: “Provide a detailed description of the person’s facial features.”

7 Extensions and Generalization

7.1 Evaluation on LADN Dataset

To further verify the generalization capability and robustness of **Adv-TGD**, we conducted additional experiments on the LADN dataset [11]. Unlike the aligned CelebA-HQ dataset, LADN contains images with significant variations in makeup, lighting, and pose, presenting a more challenging “in-the-wild” scenario. As reported in Table 4, **Adv-TGD** achieves consistently strong attack performance across all evaluated face recognition models under these challenging conditions.

Table 4. Attack Success Rate (ASR%) on the LADN dataset. Comparison against state-of-the-art methods.

Method	IR152	IRSE50	FaceNet	MobileFace
Clean	3.71	2.79	0.60	5.12
Clip2Protect	54.31	88.57	49.91	78.94
DiffAM	66.68	91.26	66.16	88.68
DiffAIM	74.21	92.67	68.44	83.45
Adv-TGD (Ours)	90.80	94.30	65.71	92.80

7.2 Extension to General Object Classification

To demonstrate the universality of the proposed **Adv-TGD** framework beyond face recognition, we extended our approach to attack general image classification models.

7.2.1 Experimental Setup. For this extension, we adapted the pipeline to target a pre-trained **ResNet-50** classifier. Instead of SGSM, we utilized class-activation maps (CAM) to derive the saliency signal, allowing the diffusion model to modify global semantic features relevant to the target class while preserving the structural essence of the source object. Text guidance was adjusted to describe the target ImageNet category (e.g., “A photo of a Golden Retriever”).

7.2.2 Qualitative Results. Fig. 8 illustrates the adversarial examples generated by **Adv-TGD** on ImageNet samples. As observed, the framework successfully injects subtle semantic features of the target class while maintaining the overall spatial structure of the source object.

7.3 Generalization Across Architectures

A core strength of the **Adv-TGD** framework is its architectural agnosticism. While our primary experiments utilize Stable Diffusion 2.1, the underlying mechanism is transferable to diverse generative and discriminative backbones.

7.3.1 Stable Diffusion 1.5 (SD 1.5). Stable Diffusion 1.5 relies on a similar UNet-based architecture but utilizes a different text encoder. The transition is seamless, and the **SGSM** strategy remains identical. We observed that Adv-TGD achieves similar or slightly higher ASR on SD 1.5 compared to SD 2.1, suggesting the vulnerability is inherent to continuous latent representations of identity. Quantitative results for different masking strategies on SD 1.5 are provided in Table 5.

Table 5. Performance of Adv-TGD masking variants on Stable Diffusion 1.5.

Variant	ASR (%) ↑	PSNR ↑	SSIM ↑
Saliency Mask	69.00	15.63	0.756
Full Image Editing	84.00	15.42	0.744
Geometric Mask (Parsing)	86.80	15.52	0.749
SGSM (Ours)	87.50	15.71	0.759

Table 6. Performance of Adv-TGD masking variants on the FLUX.1 architecture.

Variant	ASR (%) ↑	PSNR ↑	SSIM ↑
Saliency Mask	66.50	29.85	0.986
Full Image Editing	84.00	26.40	0.955
Geometric Mask (Parsing)	79.00	29.15	0.980
SGSM (Ours)	82.50	29.30	0.982

7.3.2 Flux.1 (Transformer-Based Flow Matching). To evaluate the architectural agnosticism of **Adv-TGD**, we adapted the framework to the state-of-the-art **FLUX.1-dev** model. This transition required a fundamental shift in the optimization objective, latent handling, and noise regularization to accommodate a non-UNet architecture operating via rectified flow:

- **Rectified Flow Objective:** Unlike the epsilon-prediction used in our primary experiments, FLUX utilizes a flow-matching formulation. We reformulated our MSE loss to target the velocity vector v , where the transformer predicts the linear trajectory between the source latent and random noise: $\mathcal{L}_{mse} = \|\hat{v}_\theta - (\epsilon - z_{src})\|^2$. This rectified flow training provides significantly higher gradient stability during the identity shift.

- **Dynamic Timestep Sampling:** Continuous flow-matching models are highly susceptible to “latent burn-in” if gradients are backpropagated through a fixed noise level. To ensure the adversarial identity features are robust and generalize the flow trajectory, we replaced the fixed timestep anchor with dynamic sampling $t \sim \mathcal{U}(0.2, 0.5)$. This forces the transformer to learn structural semantic shifts rather than exploiting a specific noise manifold.
- **Sequence-Spatial Mapping and Pixel-Space Masking:** Since the **Multimodal Diffusion Transformer (MMDiT)** operates on flattened 2×2 patch sequences, we implemented differentiable pack and unpack operations. Crucially, we found that applying our facial mask in the latent space introduces severe VAE decoding artifacts in FLUX. Therefore, we extract the flow predictions, fully decode them to the spatial pixel domain, and apply a strict landmark-bounded Parsing Mask (Method F) *before* FR feature extraction.
- **High-Frequency Artifact Suppression:** Massive transformer backbones have a tendency to achieve adversarial success by injecting high-frequency static rather than purely structural identity changes, which can degrade visual fidelity. While our dual-constraint perceptual regularization ($\mathcal{L}_{reg} = \lambda_{tv} \mathcal{L}_{TV} + \lambda_{lrips} \mathcal{L}_{LPIPS}$) helps suppress this, we observe that transformer-based flow matching still exhibits a higher baseline of pixel-level noise compared to UNet architectures.
- **Transformer LoRA Injection:** We localized the trainable parameters to the transformer’s cross-attention projections (`to_q`, `to_k`, `to_v`, `to_out.0`). While this enables strong semantic identity manipulation, the resulting gradients in the transformer space tend to produce rougher skin textures compared to the smooth synthesis of SD 2.1.

As shown in Table 6, adapting the framework to FLUX.1 successfully yields strong attack transferability while capitalizing on the transformer backbone to achieve high visual fidelity (PSNR ~ 29 dB, SSIM > 0.98). A core strength of the **Adv-TGD** framework is its architectural agnosticism. While our primary experiments utilize Stable Diffusion 2.1, the underlying mechanism is transferable to diverse generative backbones. As illustrated in Fig. 9, Adv-TGD produces consistent adversarial identity transformations across multiple architectures, including UNet-based diffusion models (Stable Diffusion 1.5 and 2.1) and transformer-based generative models (FLUX.1).

8 Conclusion

We introduced *Adv-TGD*, a text-guided, per-pair LoRA framework for adversarial face synthesis built on a frozen Stable Diffusion 2.1 backbone. By introducing *Salience-Guided Semantic Masking (SGSM)* and a unified identity objective—comprising ensemble hinges, directional guidance, and source suppression—*Adv-TGD* enables targeted identity manipulation that is both parameter-efficient and structurally consistent. Unlike traditional adversarial noise, our method targets low-to-mid frequency facial features to neutralize recognizers by dispersing their spatial attention. Extensive experiments on CelebA-HQ and FFHQ under a strict black-box setting demonstrate that *Adv-TGD* achieves exceptional transferability across industry-standard FR models. Our method attains a state-of-the-art mean ASR of **85.90%**, outperforming representative noise-based, makeup-based, and semantic baselines. Crucially, *Adv-TGD* maintains superior pixel-level perceptual quality, achieving a PSNR of 27.15 dB and an SSIM of 0.981, ensuring that the adversarial faces remain photorealistic and structurally faithful to the source context. Our results reveal a previously underexplored vulnerability of modern face recognition systems to generative diffusion-based attacks. By combining semantic guidance and localized identity manipulation, Adv-TGD achieves strong impersonation success while preserving high perceptual realism. These findings highlight the need for more robust biometric systems capable of defending against generative

adversarial attacks. Beyond academic face recognition benchmarks, we demonstrated the framework’s broad universality and architectural agnosticism. Evaluations on commercial systems (Face++), in-the-wild datasets (LADN), and general object classification (ImageNet) confirm its robust real-world applicability. Furthermore, cross-architecture validations on Stable Diffusion 1.5 and the state-of-the-art transformer-based FLUX.1 model highlight that the fusion of semantic constraints with target-aware saliency is highly adaptable. Overall, our results demonstrate that text-guided localized generative adaptation offers an explainable, practical, and highly effective paradigm for adversarial impersonation against unauthorized recognition.

References

- [1] Denise Almeida, Konstantin Shmarko, and Elizabeth Lomas. 2022. The ethics of facial recognition technologies, surveillance, and accountability in an age of artificial intelligence: a comparative analysis of US, EU, and UK regulatory frameworks. *AI and Ethics* 2, 3 (2022), 377–387.
- [2] Yogesh Balaji, Seungjun Nah, Xun Huang, Arash Vahdat, Jiaming Song, Qinheng Zhang, Karsten Kreis, Miika Aittala, Timo Aila, Samuli Laine, et al. 2022. ediff-i: Text-to-image diffusion models with an ensemble of expert denoisers. *arXiv preprint arXiv:2211.01324* (2022).
- [3] Valeriia Cherepanova, Micah Goldblum, Harrison Foley, Shiyuan Duan, John Dickerson, Gavin Taylor, and Tom Goldstein. 2021. Lowkey: Leveraging adversarial attacks to protect social media users from facial recognition. *arXiv preprint arXiv:2101.07922* (2021).
- [4] Saheb Chhabra, Kartik Thakral, Richa Singh, and Mayank Vatsa. 2025. PrIdentity: Generalizable Privacy Preserving Adversarial Perturbations for Anonymizing Facial Identity. *IEEE Transactions on Biometrics, Behavior, and Identity Science* (2025).
- [5] Ka-Ho Chow, Sihao Hu, Tiansheng Huang, and Ling Liu. 2024. Personalized privacy protection mask against unauthorized facial recognition. In *European Conference on Computer Vision*. Springer, 434–450.
- [6] Prafulla Dhariwal and Alexander Nichol. 2021. Diffusion models beat gans on image synthesis. *Advances in neural information processing systems* 34 (2021), 8780–8794.
- [7] Yinpeng Dong, Fangzhou Liao, Tianyu Pang, Hang Su, Jun Zhu, Xiaolin Hu, and Jianguo Li. 2018. Boosting adversarial attacks with momentum. In *Proceedings of the IEEE conference on computer vision and pattern recognition*. 9185–9193.
- [8] Yinpeng Dong, Tianyu Pang, Hang Su, and Jun Zhu. 2019. Evading defenses to transferable adversarial examples by translation-invariant attacks. In *Proceedings of the IEEE/CVF conference on computer vision and pattern recognition*. 4312–4321.
- [9] Yanbo Fan, Baoyuan Wu, Tuanhui Li, Yong Zhang, Mingyang Li, Zhifeng Li, and Yujiu Yang. 2020. Sparse adversarial attack via perturbation factorization. In *European conference on computer vision*. Springer, 35–50.
- [10] Weiwei Feng, Nanqing Xu, Tianzhu Zhang, and Yongdong Zhang. 2023. Dynamic generative targeted attacks with pattern injection. In *Proceedings of the IEEE/CVF Conference on Computer Vision and Pattern Recognition*. 16404–16414.
- [11] Qiao Gu, Guanzhi Wang, Mang Tik Chiu, Yu-Wing Tai, and Chi-Keung Tang. 2019. Ladrn: Local adversarial disentangling network for facial makeup and de-makeup. In *Proceedings of the IEEE/CVF International Conference on Computer Vision*. 10481–10490.
- [12] Martin Heusel, Hubert Ramsauer, Thomas Unterthiner, Bernhard Nessler, and Sepp Hochreiter. 2017. Gans trained by a two time-scale update rule converge to a local nash equilibrium. *Advances in neural information processing systems* 30 (2017).
- [13] Jonathan Ho, Ajay Jain, and Pieter Abbeel. 2020. Denoising Diffusion Probabilistic Models. In *Advances in Neural Information Processing Systems*.
- [14] Edward J Hu, Yelong Shen, Phillip Wallis, Zeyuan Allen-Zhu, Yuanzhi Li, Shean Wang, Liang Wang, Weizhu Chen, et al. 2022. Lora: Low-rank adaptation of large language models. *Iclr* (2022).
- [15] Shengshan Hu, Xiaogeng Liu, Yechao Zhang, Minghui Li, Leo Yu Zhang, Hai Jin, and Libing Wu. 2022. Protecting facial privacy: Generating adversarial identity masks via style-robust makeup transfer. In *Proceedings of the IEEE/CVF conference on computer vision and pattern recognition*. 15014–15023.
- [16] Lianghua Huang, Di Chen, Yu Liu, Yujun Shen, Deli Zhao, and Jingren Zhou. 2023. Composer: creative and controllable image synthesis with composable conditions. In *Proceedings of the 40th International Conference on Machine Learning (Honolulu, Hawaii, USA) (ICML ’23)*. JMLR.org, Article 558, 21 pages.
- [17] Zhizhong Huang, Shouzhen Chen, Junping Zhang, and Hongming Shan. 2020. PFA-GAN: Progressive face aging with generative adversarial network. *IEEE Transactions on Information Forensics and Security* 16 (2020), 2031–2045.
- [18] Shuai Jia, Bangjie Yin, Taiping Yao, Shouhong Ding, Chunhua Shen, Xiaokang Yang, and Chao Ma. 2022. Adv-attribute: Inconspicuous and transferable adversarial attack on face recognition. *Advances in Neural Information Processing Systems* 35 (2022), 34136–34147.
- [19] Cemre Efe Karakas, Alara Dirik, Eylül Yalçinkaya, and Pinar Yanardag. 2022. Fairstyle: Debiasing stylegan2 with style channel manipulations. In *European Conference on Computer Vision*. Springer, 570–586.
- [20] Tero Karras, Timo Aila, Samuli Laine, and Jaakko Lehtinen. 2017. Progressive growing of gans for improved quality, stability, and variation. *arXiv preprint arXiv:1710.10196* (2017).
- [21] Tero Karras, Samuli Laine, and Timo Aila. 2019. A style-based generator architecture for generative adversarial networks. In *Proceedings of the IEEE/CVF conference on computer vision and pattern recognition*. 4401–4410.

- [22] Minchul Kim, Feng Liu, Anil Jain, and Xiaoming Liu. 2023. Dcfac: Synthetic face generation with dual condition diffusion model. In *Proceedings of the IEEE/CVF conference on computer vision and pattern recognition*. 12715–12725.
- [23] Stepan Komkov and Aleksandr Petiushko. 2021. Advhat: Real-world adversarial attack on arcface face id system. In *2020 25th international conference on pattern recognition (ICPR)*. IEEE, 819–826.
- [24] Nupur Kumari, Bingliang Zhang, Richard Zhang, Eli Shechtman, and Jun-Yan Zhu. 2023. Multi-concept customization of text-to-image diffusion. In *Proceedings of the IEEE/CVF conference on computer vision and pattern recognition*. 1931–1941.
- [25] Wenyun Li, Zheng Zhang, Xiangyuan Lan, and Dongmei Jiang. 2025. Transferable adversarial face attack with text controlled attribute. In *Proceedings of the AAAI Conference on Artificial Intelligence*, Vol. 39. 4977–4985.
- [26] Decheng Liu, Xijun Wang, Chunlei Peng, Nannan Wang, Ruimin Hu, and Xinbo Gao. 2024. Adv-diffusion: imperceptible adversarial face identity attack via latent diffusion model. In *Proceedings of the AAAI conference on artificial intelligence*, Vol. 38. 3585–3593.
- [27] Jiang Liu, Chun Pong Lau, and Rama Chellappa. 2023. Diffprotect: Generate adversarial examples with diffusion models for facial privacy protection. *arXiv preprint arXiv:2305.13625* (2023).
- [28] Yunfan Liu, Qi Li, Qiyao Deng, Zhenan Sun, and Ming-Hsuan Yang. 2023. Gan-based facial attribute manipulation. *IEEE transactions on pattern analysis and machine intelligence* 45, 12 (2023), 14590–14610.
- [29] Haotian Ma, Ke Xu, Xinghao Jiang, Zeyu Zhao, and Tanfeng Sun. 2023. Transferable black-box attack against face recognition with spatial mutable adversarial patch. *IEEE Transactions on Information Forensics and Security* 18 (2023), 5636–5650.
- [30] Aleksander Madry, Aleksandar Makelov, Ludwig Schmidt, Dimitris Tsipras, and Adrian Vladu. 2018. Towards Deep Learning Models Resistant to Adversarial Attacks. In *International Conference on Learning Representations (ICLR)*.
- [31] Yuxi Mi, Zhizhou Zhong, Yuge Huang, Jiazhen Ji, Jianqing Xu, Jun Wang, Shaoming Wang, Shouhong Ding, and Shuigeng Zhou. 2024. Privacy-preserving face recognition using trainable feature subtraction. In *Proceedings of the IEEE/CVF Conference on Computer Vision and Pattern Recognition*. 297–307.
- [32] Vahid Mirjalili, Sebastian Raschka, and Arun Ross. 2020. PrivacyNet: Semi-adversarial networks for multi-attribute face privacy. *IEEE Transactions on Image Processing* 29 (2020), 9400–9412.
- [33] Chong Mou, Hongzhi Ye, Jiaming Li, Ailin Zeng, Yang Cao, Qiang Xu, Lewei Lu, and Jifeng Zhu. 2023. T2I-Adapters: Learning Adapters to Dig out More Controllable Ability for Text-to-Image Diffusion Models. In *IEEE International Conference on Computer Vision (ICCV)*.
- [34] Cristian Muñoz, Sara Zannone, Umar Mohammed, and Adriano Koshiyama. 2023. Uncovering bias in face generation models. *arXiv preprint arXiv:2302.11562* (2023).
- [35] Alex Nichol, Prafulla Dhariwal, Aditya Ramesh, Pranav Shyam, Pamela Mishkin, Bob McGrew, Ilya Sutskever, and Mark Chen. 2021. Glide: Towards photorealistic image generation and editing with text-guided diffusion models. *arXiv preprint arXiv:2112.10741* (2021).
- [36] Malsha V Perera and Vishal M Patel. 2025. Unbiased-Diff: Analyzing and Mitigating Biases in Diffusion Model-Based Face Image Generation. *IEEE Transactions on Biometrics, Behavior, and Identity Science* (2025).
- [37] Jiatian Pi, Junyi Zeng, Quan Lu, Ning Jiang, Haiying Wu, Linchengxi Zeng, and Zhiyou Wu. 2023. Adv-Eye: A Transfer-Based Natural Eye Makeup Attack on Face Recognition. *IEEE Access* 11 (2023), 89369–89382. doi:10.1109/ACCESS.2023.3307132
- [38] Nicolas Pinto, Zak Stone, Todd Zickler, and David Cox. 2011. Scaling up biologically-inspired computer vision: A case study in unconstrained face recognition on facebook. In *CVPR 2011 workshops*. IEEE, 35–42.
- [39] David Podell et al. 2023. SDXL: Improving Latent Diffusion Models for High-Resolution Image Synthesis. *arXiv preprint arXiv:2307.01952*.
- [40] Aditya Ramesh, Prafulla Dhariwal, Alex Nichol, Casey Chu, and Mark Chen. 2022. Hierarchical text-conditional image generation with clip latents. *arXiv preprint arXiv:2204.06125* (2022).
- [41] Robin Rombach, Andreas Blattmann, Dominik Lorenz, Patrick Esser, and Björn Ommer. 2022. High-Resolution Image Synthesis with Latent Diffusion Models. In *IEEE Conference on Computer Vision and Pattern Recognition (CVPR)*.
- [42] Robin Rombach, Andreas Blattmann, Dominik Lorenz, Patrick Esser, and Björn Ommer. 2022. High-resolution image synthesis with latent diffusion models. In *Proceedings of the IEEE/CVF conference on computer vision and pattern recognition*. 10684–10695.
- [43] Chitwan Saharia, William Chan, Saurabh Saxena, Lala Li, Jay Whang, Emily L Denton, Kamyar Ghasemipour, Raphael Gontijo Lopes, Burcu Karagol Ayan, Tim Salimans, et al. 2022. Photorealistic text-to-image diffusion models with deep language understanding. *Advances in neural information processing systems* 35 (2022), 36479–36494.
- [44] Fahad Shamshad, Muzammal Naseer, and Karthik Nandakumar. 2023. Clip2protect: Protecting facial privacy using text-guided makeup via adversarial latent search. In *Proceedings of the IEEE/CVF Conference on Computer Vision and Pattern Recognition*. 20595–20605.
- [45] Fahad Shamshad, Muzammal Naseer, and Karthik Nandakumar. 2024. Makeup-guided facial privacy protection via untrained neural network priors. In *European Conference on Computer Vision*. Springer, 227–246.
- [46] Shawn Shan, Emily Wenger, Jiayun Zhang, Huiying Li, Haitao Zheng, and Ben Y Zhao. 2020. Fawkes: Protecting privacy against unauthorized deep learning models. In *29th USENIX security symposium (USENIX Security 20)*. 1589–1604.
- [47] Yang Song, Jascha Sohl-Dickstein, Diederik P Kingma, Abhishek Kumar, Stefano Ermon, and Ben Poole. 2021. Score-Based Generative Modeling through Stochastic Differential Equations. In *International Conference on Learning Representations*.
- [48] Michał Stypulkowski, Konstantinos Vougioukas, Sen He, Maciej Zięba, Stavros Petridis, and Maja Pantic. 2024. Diffused heads: Diffusion models beat gans on talking-face generation. In *Proceedings of the IEEE/CVF Winter Conference on Applications of Computer Vision*. 5091–5100.

- [49] Yuhao Sun, Lingyun Yu, Hongtao Xie, Jiaming Li, and Yongdong Zhang. 2024. Diffam: Diffusion-based adversarial makeup transfer for facial privacy protection. In *Proceedings of the IEEE/CVF conference on computer vision and pattern recognition*. 24584–24594.
- [50] Chien-Yi Wang, Yu-Ding Lu, Shang-Ta Yang, and Shang-Hong Lai. 2022. Patchnet: A simple face anti-spoofing framework via fine-grained patch recognition. In *Proceedings of the IEEE/CVF conference on computer vision and pattern recognition*. 20281–20290.
- [51] Junying Wang, Hongyuan Zhang, and Yuan Yuan. 2025. Adv-cpg: A customized portrait generation framework with facial adversarial attacks. In *Proceedings of the Computer Vision and Pattern Recognition Conference*. 21001–21010.
- [52] Liqin Wang, Qianyue Hu, Wei Lu, and Xiangyang Luo. 2025. Diffusion-based adversarial identity manipulation for facial privacy protection. In *Proceedings of the 33rd ACM International Conference on Multimedia*. 11562–11571.
- [53] Tianyi Wang, Shuaicheng Niu, Harry Cheng, Xiao Zhang, and Yinglong Wang. 2025. Nullswap: Proactive identity cloaking against deepfake face swapping. In *Proceedings of the IEEE/CVF International Conference on Computer Vision*. 9945–9954.
- [54] Zhibo Wang, He Wang, Shuaifan Jin, Wenwen Zhang, Jiahui Hu, Yan Wang, Peng Sun, Wei Yuan, Kaixin Liu, and Kui Ren. 2023. Privacy-preserving adversarial facial features. In *Proceedings of the IEEE/CVF Conference on Computer Vision and Pattern Recognition*. 8212–8221.
- [55] Xingxing Wei, Ying Guo, and Jie Yu. 2022. Adversarial sticker: A stealthy attack method in the physical world. *IEEE Transactions on Pattern Analysis and Machine Intelligence* 45, 3 (2022), 2711–2725.
- [56] Xingxing Wei, Ying Guo, Jie Yu, and Bo Zhang. 2022. Simultaneously optimizing perturbations and positions for black-box adversarial patch attacks. *IEEE transactions on pattern analysis and machine intelligence* 45, 7 (2022), 9041–9054.
- [57] Xingxing Wei, Caixin Kang, Yinpeng Dong, Zhengyi Wang, Shouwei Ruan, Yubo Chen, and Hang Su. 2025. Real-world adversarial defense against patch attacks based on diffusion model. *IEEE Transactions on Pattern Analysis and Machine Intelligence* (2025).
- [58] Xingxing Wei, Shouwei Ruan, Yinpeng Dong, Hang Su, and Xiaochun Cao. 2025. Distributionally location-aware transferable adversarial patches for facial images. *IEEE Transactions on Pattern Analysis and Machine Intelligence* 47, 4 (2025), 2849–2864.
- [59] Emily Wenger, Shawn Shan, Haitao Zheng, and Ben Y Zhao. 2023. Sok: Anti-facial recognition technology. In *2023 IEEE Symposium on Security and Privacy (SP)*. IEEE, 864–881.
- [60] Zhenyu Wu, Zhangyang Wang, Zhaowen Wang, and Hailin Jin. 2018. Towards privacy-preserving visual recognition via adversarial training: A pilot study. In *Proceedings of the European conference on computer vision (ECCV)*. 606–624.
- [61] Xiao Yang, Yinpeng Dong, Tianyu Pang, Hang Su, Jun Zhu, Yuefeng Chen, and Hui Xue. 2021. Towards face encryption by generating adversarial identity masks. In *Proceedings of the IEEE/CVF international conference on computer vision*. 3897–3907.
- [62] Xiao Yang, Chang Liu, Longlong Xu, Yikai Wang, Yinpeng Dong, Ning Chen, Hang Su, and Jun Zhu. 2023. Towards effective adversarial textured 3d meshes on physical face recognition. In *Proceedings of the IEEE/CVF conference on computer vision and pattern recognition*. 4119–4128.
- [63] Bangjie Yin, Wenxuan Wang, Taiping Yao, Junfeng Guo, Zelun Kong, Shouhong Ding, Jilin Li, and Cong Liu. 2021. Adv-makeup: A new imperceptible and transferable attack on face recognition. *arXiv preprint arXiv:2105.03162* (2021).
- [64] Hao Yu, Margrit Betke, and Sarah Adel Bargal. 2025. Data Bias Mitigation and Evaluation Framework for Diffusion-based Generative Face Models. In *Proceedings of the IEEE/CVF International Conference on Computer Vision*. 300–310.
- [65] Zhanpeng Zhang, Ping Luo, Chen Change Loy, and Xiaoou Tang. 2018. From facial expression recognition to interpersonal relation prediction. *International Journal of Computer Vision* 126, 5 (2018), 550–569.
- [66] Zheng-An Zhu, Yun-Zhong Lu, and Chen-Kuo Chiang. 2019. Generating adversarial examples by makeup attacks on face recognition. In *2019 IEEE International Conference on Image Processing (ICIP)*. IEEE, 2516–2520.

9 Ethical Considerations

Our research explores vulnerabilities in face recognition systems using generative AI. While the proposed Adv-TGD framework can synthesize impersonation images, we emphasize that this work is intended for defensive security analysis and privacy protection. All experiments were conducted using publicly available research datasets (CelebA-HQ, FFHQ, LADN). We do not release any pre-trained LoRA weights for specific individuals, and our methodology is designed to inform the development of more robust biometric verification systems against generative threats.

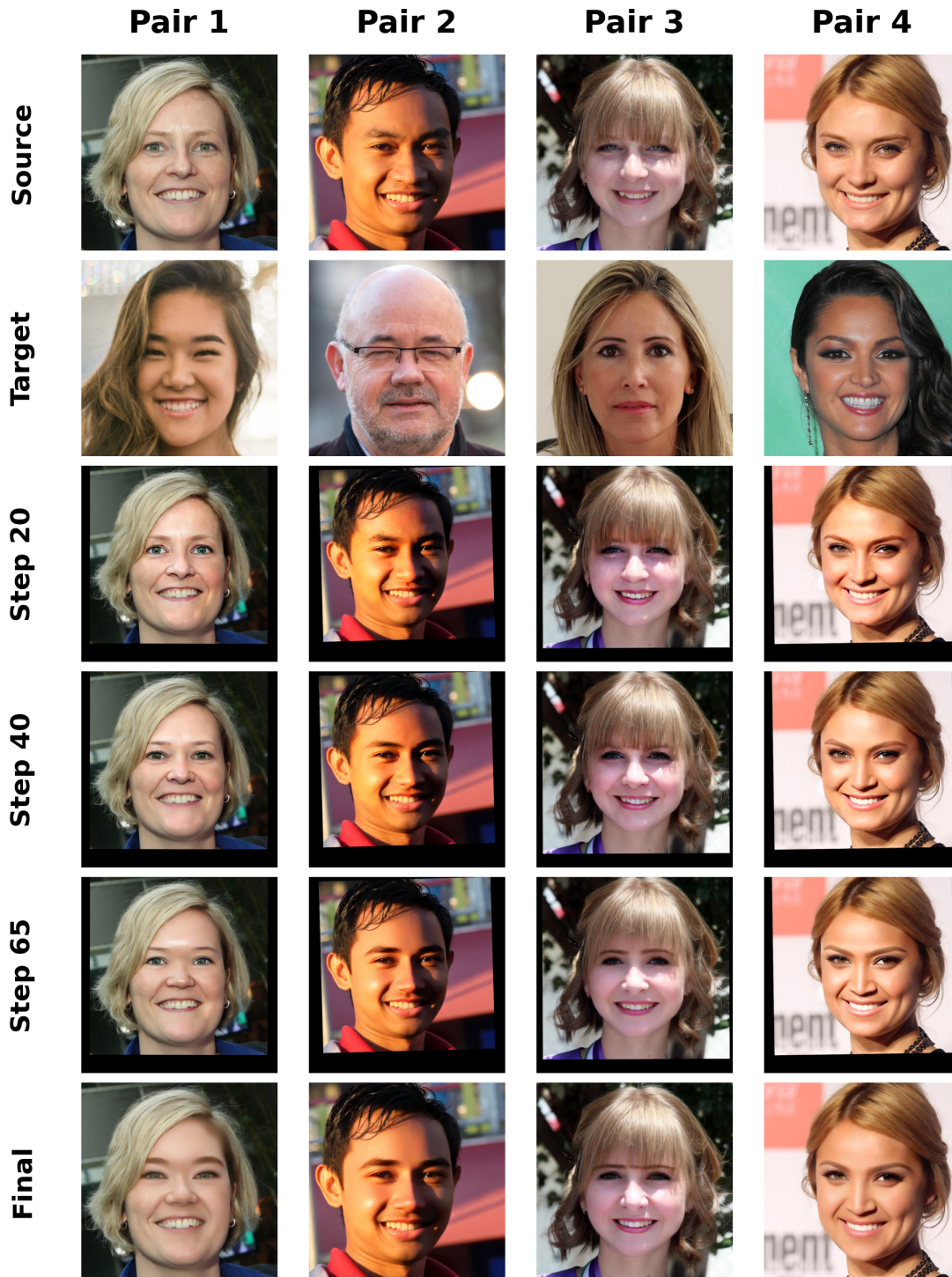


Fig. 6. **Evolution of the Adversarial Identity.** Visualization of the Adv-TGD optimization process across different steps. The source face gradually adopts the structural and semantic features of the target identity over iterations, culminating in a seamlessly blended final output.



A woman with fair skin, brown eyes, arched eyebrows, a straight nose, and a thin mouth



A man with a square face, light skin, blue eyes, thin eyebrows, a straight nose, a thin mouth, and glasses

Fig. 7. Example texts used during the late-stage guidance phase.

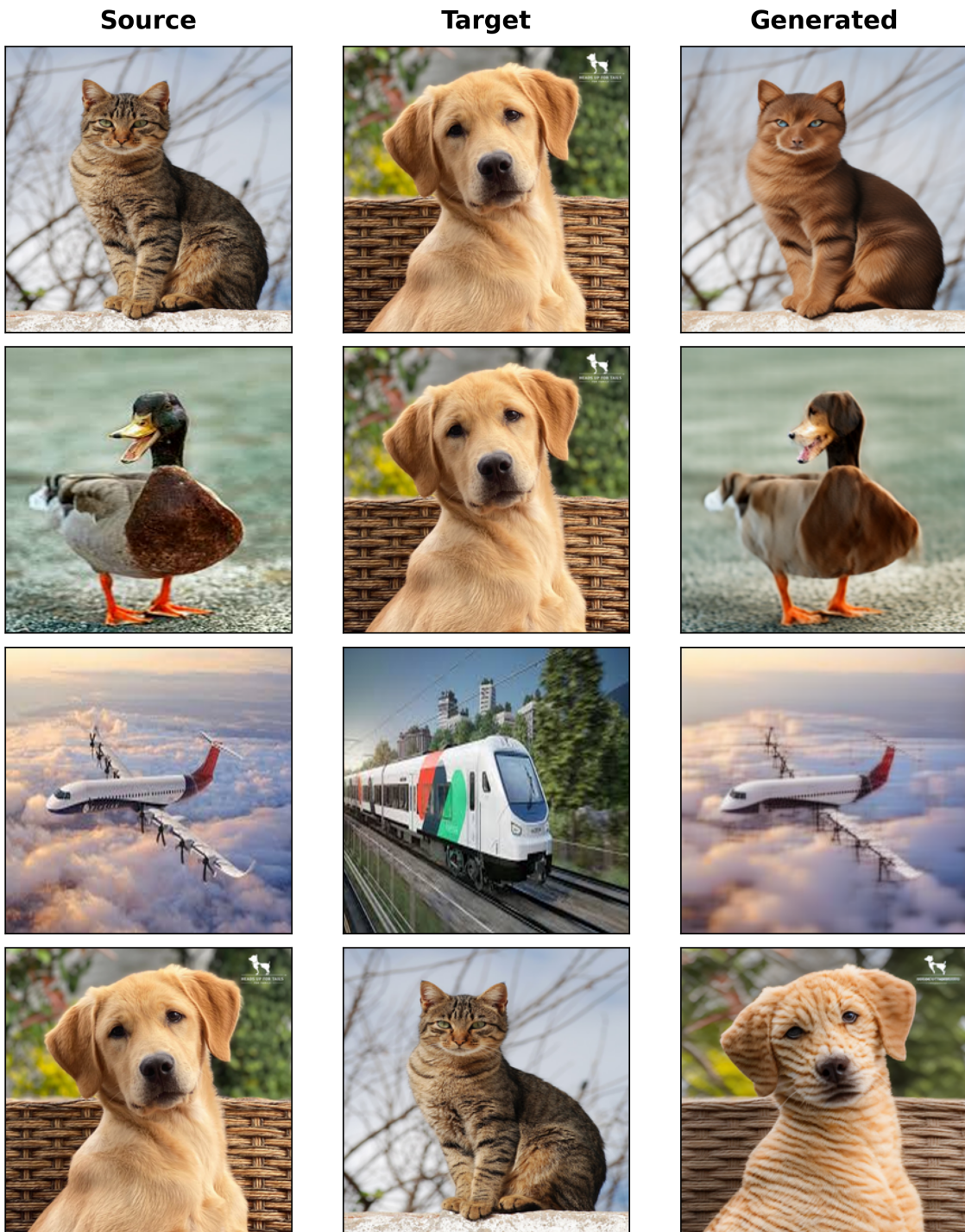


Fig. 8. **General Object Classification Attack.** Qualitative results of Adv-TGD attacking a ResNet-50 classifier on ImageNet. Manuscript submitted to ACM

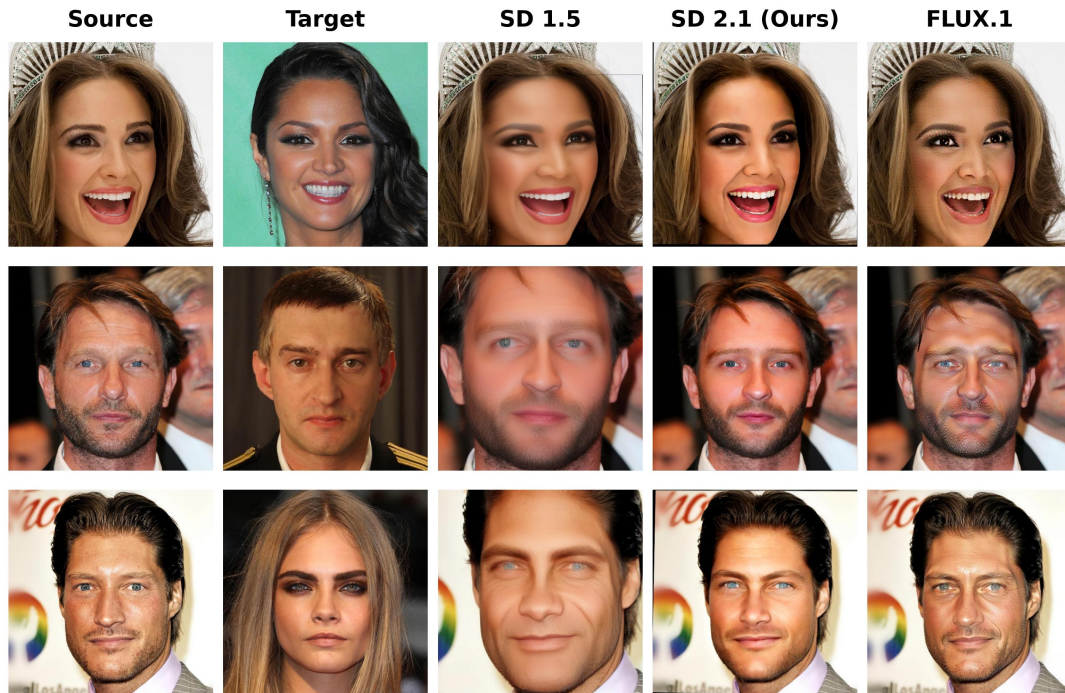


Fig. 9. **Cross-Architecture Generalization.** Visual comparison of Adv-TGD generated adversarial faces across different generative backbones. From left to right: Source, Target, Stable Diffusion 1.5, Stable Diffusion 2.1 (Primary), and FLUX.1. The framework consistently achieves robust identity transfer and structural preservation.